

pH-responsive amphiphilic block copolymer prodrug conjugated near infrared fluorescence probe

Cite this: *RSC Adv.*, 2014, 4, 28186

Tao Xing and Lifeng Yan*

A novel amphiphilic multi-block copolymer conjugated with both a near infrared fluorescence probe and drug has been designed and prepared by means of ring-opening polymerization (ROP) of *N*-Carboxy Anhydride (NCA) monomers following a Reversible Addition-Fragmentation Chain Transfer (RAFT) polymerization. At first, an amino group-containing RAFT agent was synthesized and it served as an initiator for the sequential ROP of aspartic acid β -benzyl ester *N*-carboxy anhydride (Asp-NCA) and ϵ -carbobenzoxy-L-lysine NCA (ZLLys-NCA). Then the multi-block copolymer was prepared by a succeeding RAFT polymerization of poly(ethylene glycol) methyl ether acrylate (OGEA). At the end, both anticancer drug doxorubicin and hydrophobic aminocyanine dye were chemical conjugated to the block copolymer *via* a hydrazone or amide bond, respectively. The obtained NIRF copolymer and its micelles were characterized by nuclear magnetic resonance (NMR), gel permeation chromatography (GPC), dynamic light scattering (DLS), and UV-vis and fluorescence spectrophotometry. The prodrug has strong fluorescence in the near infrared region and shows pH-responsive drug release behavior, and it has potential application in the theranostics of cancer.

Received 12th May 2014

Accepted 9th June 2014

DOI: 10.1039/c4ra04423a

www.rsc.org/advances

Introduction

For cancer treatment, both diagnosis and subsequent therapy are important, and theranosis has been attracted much attention, recently.^{1,2} A drug delivery system with bioimaging ability also affords the possibility of a precise location of the drug carrier, providing useful information both for the diagnosis of disease and its subsequent treatment. Incorporating various bioimaging agents such as quantum dots,^{3,4} iron oxide,⁵⁻⁷ radionuclide agents⁸ and organic dyes⁹⁻¹¹ into nanocarrier have performed for these purposes. Among the various kinds of imaging methods developed, optical imaging is largely utilized because of its non-invasive nature. However, strong absorption from hemoglobin can be detected at wavelengths lower than 600 nm, and significant background fluorescence from endogenous biomolecules can be detected up to wavelengths of 680 nm.¹² Imaging in the near infrared region (NIR, >700 nm) has been widely used for live body imaging because it works in a wavelength range where body tissue has the least interference.

Cyanine dye is a type of the most widely used NIR probe as long wavelength imaging agent with commercial availability and FDA approval for clinical use.¹³ Physical encapsulation or chemical conjugation cyanine dye into the polymeric

nanocarriers provides a way to improve the dye stability because it prevents the interaction of dye with either solvent or other dye molecules. Compared with physical encapsulation, chemical conjugation of the dye molecules to the nanocarrier may be more suitable in that it prevents the dye from leakage during blood circulation. Thus prolonging the fluorescent time of the system.

Polymeric nanoparticles are potential theranostic systems for future cancer treatment due to their versatilities in both structure and functionality.^{11,14-16} Synthesis of polymeric materials with versatile structures and bioimaging groups are an ongoing area due to their potential applications in future biomedical areas.¹⁴ Amphiphilic polymers are known to self-assemble into nano-sized micelle in aqueous solution, which makes it a useful candidate for both drug delivery and cancer diagnostics. The rationale for the above two applications lies in the enhanced permeability and retention (EPR) effect of micelle or nanogel.¹⁷

Chemotherapy is an effective method for tumor treatment, but its application has been restricted owing to the lack of an effective drug delivery method to tumor tissue. Small drug molecules normally could not reach the tumor tissue efficiently and nonspecific distribution of the administered drug in biological system not only results in unwanted drug waste, but also leads to much more serious problems usually resulting from its pronounced toxicity to normal tissue. Physically or chemically loaded drug in nanoparticles could reduce drug loss during blood circulation, thus increasing drug using efficiency.^{18,19}

CAS Key Laboratory of Soft Matter Chemistry, Hefei National Laboratory for Physical Sciences at the Microscale, Department of Chemical Physics, University of Science and Technology of China, Hefei, 230026, P.R. China. E-mail: lfyang@ustc.edu.cn; Fax: +86-551-3603748; Tel: +86-551-63606853

Recently, polymeric prodrug nanogels or micelles have received much attention for they could offer several significant advantages for cancer therapy, such as improved water solubility of drugs and enhanced drug bioavailability.^{20,21} In addition, polymeric prodrugs are more stable in blood circulation since the drug is conjugated to the polymer with covalent bonds.²² The development of intelligent nanoparticles^{23–26} which could release loaded drug under environmental stimuli at a desired site further optimizes the drug performance. Usually, the drug can be chemically bonded to non-responsive nanoparticles *via* a responsive chemical bond,^{27–29} pH-responsive nanoparticles were developed on the basis of more acidic nature of tumor cell and its microenvironment.^{29,30} Usually, pH-responsive nanoparticles are required to be stable at physiological pH (7.0), but undergoes chemical bond cleavage and drug release activation under acid condition (pH = 5.0–6.0 in endocytic vesicles or 6.5–6.8 in tumor microenvironment).³¹ One meritorious example was the attachment of doxorubicin (DOX) to hydrazine containing copolymers *via* hydrazone bond, hydrolysis of the hydrazone linkage under acidic condition leads to activation of the originally dormant drug delivery system.^{28,32}

Combined a NIR dye with a pH-responsive drug-conjugated nanoparticle can be a useful method for tumor theranosis. With the aid of a NIR dye, the accumulation behavior of the nanoparticle could be conveniently monitored *in vivo*. Due to the EPR effect directed nanoparticle accumulation, NIR fluorescence signal is also hoped to accumulate at the tumor site during blood circulation. Tumor imaging could thus be realized without using the usual complicated modified cyanine molecules with tumor-targeting ability.^{33–35} Cyanine dyes can be incorporated into nanoparticle *via* chemical conjugation.^{36,37} Both hydrophobic and hydrophilic cyanine molecules could be used for nanoparticle conjugation.

In our previous studies, polypeptide nanogels or micelles with conjugated NIR probe had been synthesized for imaging the drug delivery in both *in vitro* and *in vivo*, and a long NIR image-guided drug delivery had been achieved.^{20,38–41}

Here, we reported the synthesis of a novel amphiphilic multi-block copolymer prodrug with both near infrared fluorescence and pH responsive property. Both ring-opening polymerization (ROP) of *N*-Carboxy Anhydride (NCA) monomers and reversible addition-fragmentation chain transfer (RAFT) polymerization have been involved, and both anticancer drug doxorubicin and hydrophobic aminocyanine dye were chemical conjugated to the block copolymer (Scheme 1). Micellization of the above NIRF prodrug into water leads to the formation of NIRF polymeric prodrug with both drug delivering and diagnostic abilities. Combined both pH-responsive drug release ability and near infrared optical property, the material synthesized here can be a paradigm for future theranostic application in cancer treatment.

Experimental section

Materials

All chemical agents with AR purity except specifically indicated were purchased from Sinoreagent Corporation. *n*-Hexane and

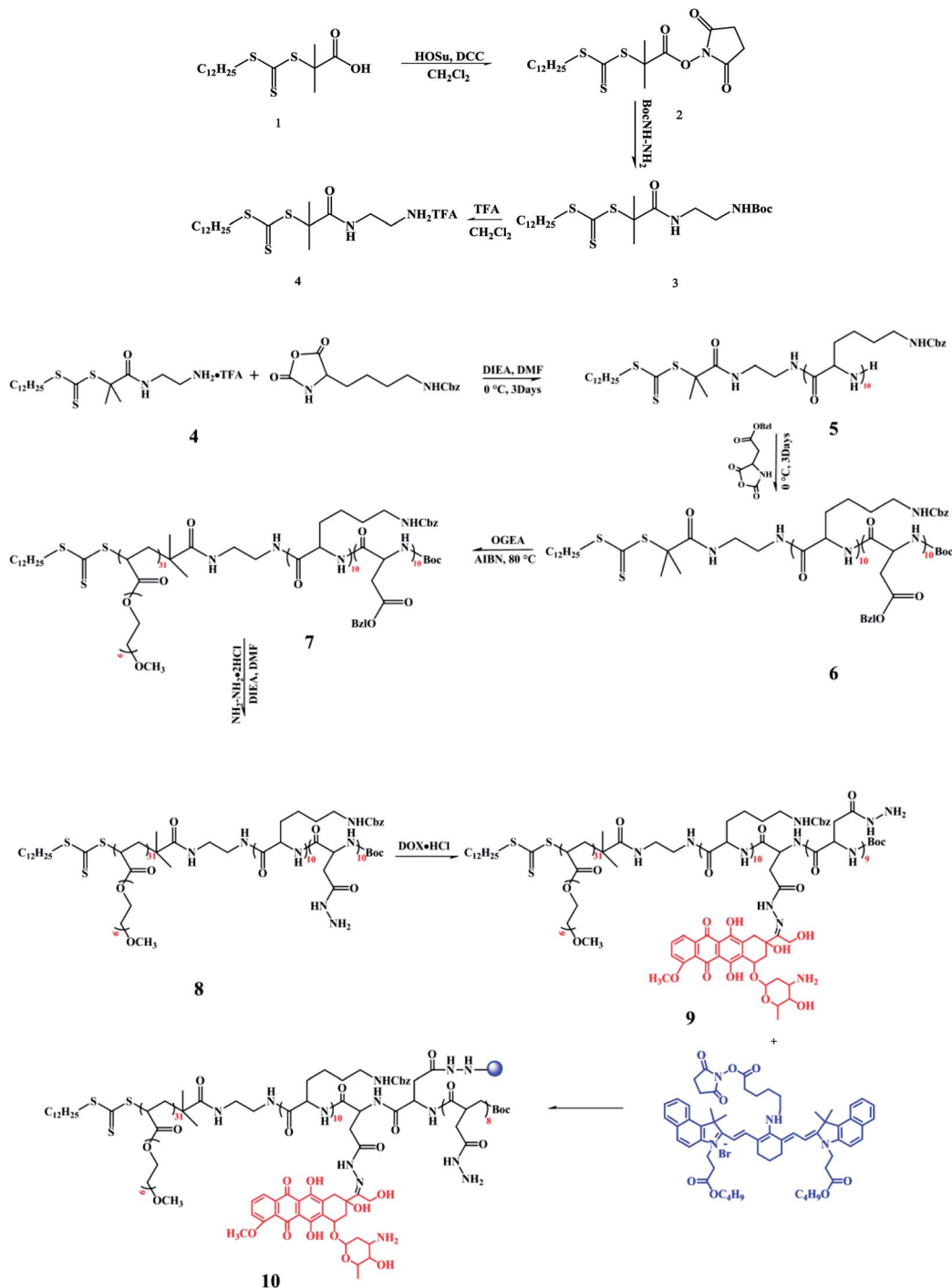
tetrahydrofuran (THF) were first refluxed with CaH₂ overnight followed by distillation. *N,N*-Dimethylformamide (DMF) was dried over CaH₂ at room temperature for 24 h before vacuum distillation. Triphosgene (99%), dichloromethane, doxorubicin hydrochloride (98%), trifluoroacetic acid, sodium acetate, hydrazine dihydrochloride (98%), 3-bromopropionic acid, *N*-hydroxysuccinimide (HOSu), *N,N'*-dicyclohexyl carbodiimide (DCC), diisopropylethylamine (DIEA), di-*tert*-butyl dicarbonate, *N*-Boc-ethylenediamine, β -benzyl *L*-aspartate, and ϵ -carbobenzoxy-*L*-lysine were purchased from Aladdin Corporation, China. Dialysis bag (cutoff $M_w = 8000$) was obtained from Bomei biotechnology corporation, China. mPEG ($M_w = 1900$) were purchased from Aldrich and used as received without further purification. Milli-Q water (18.2 M Ω) was prepared using a Milli-Q Synthesis System (Millipore, USA). Normal phase column chromatography was carried out using 200–300 mesh silica gel (Yantai institute of chemical engineering, China).

Synthesis of Llys-NCA

Llys-NCA was prepared taking a literature method.⁴² In brief, Nepsilon-carbobenzoxy-*L*-lysine (2.0 g, 7.1 mmol) was suspended in 50 mL dry THF, followed by the addition of a THF solution of triphosgene (2.1 g, 7.1 mmol). Next, the obtained suspension was stirred at 45 °C for 2 h, followed by filtration to remove traces unreacted Nepsilon-carbobenzoxy-*L*-lysine, and the filtrate was collected and crystallized three times from a mixture of THF and hexane to give the anhydride as white crystals (1.6 g, 73% yields). ¹H NMR (300 MHz, CDCl₃, δ , ppm) δ 7.48 (s, 5H), 6.75 (s, 1H), 5.42–5.13 (m, 2H), 5.01 (s, 1H), 4.40 (s, 1H), 3.32 (d, $J = 5.5$ Hz, 2H), 2.23–1.40 (m, 6H). ¹³C NMR (300 MHz, DMSO, δ , ppm): δ 171.8, 156.1, 152.0, 137.3, 128.4, 127.8, 65.1, 57.0, 41.3, 31.1, 30.6, 28.7. FT-IR (KBr, thin film, cm⁻¹): 1785, 1854.

Synthesis of RAFT agent 2 and 3

2.0 g (5.5 mmol) of RAFT agent 1 was dissolved into 50 mL of dried CH₂Cl₂, and the obtained yellow solution was cooled in an ice bath. Then, 20 mL CH₂Cl₂ containing of 1.50 g (7.3 mmol) of DCC and 0.76 g (6.6 mmol) of HOSu were added and the mixture was stirred for 36 h, and a white suspension was obtained (RAFT agent 2). After removing the precipitate, the solution was cooled down to -10 °C, and 0.73 g (5.5 mmol) of *N*-Boc-ethylenediamine was added, and the mixture was kept 0 °C overnight. After the solvent was removed under vacuum, the obtained oil residue was purified by column chromatography using a mixture of petroleum ether and ethyl acetate (5 : 1) as eluent. At the end, 2.1 g of a yellow oil-like product was obtained (78% yields). ¹H NMR (400 MHz, CDCl₃, δ , ppm): 0.88 (t, 3H, CH₃), 1.25–1.67 (m, 20H, CH₂), 1.43 (s, 9H, CH₃), 1.72 (s, 6H, CH₃), 3.23–3.34 (m, 6H, CH₂). ¹³C NMR (400 MHz, CDCl₃, δ , ppm) 14.06, 22.61, 25.70, 27.62, 28.31, 28.90, 29.01, 29.26, 29.36, 29.46, 29.54, 31.83, 37.02, 39.86, 40.98, 56.95, 79.38, 156.40, 173.02, 220.71.



Scheme 1 Synthesis of NIRF pH-responsive polymeric prodrug via a combination of ROP and RAFT polymerization.

Synthesis of RAFT agent 4

0.5 g of the as-prepared RAFT agent **3** was dissolved in 2.0 mL of trifluoroacetic acid, and it was stirred for 1 h at room temperature. Then the solvent was removed under vacuum, and the obtained oil residue was purified by column chromatography using a mixture of ethyl acetate and methanol (10 : 1) as eluent. After the solvent was removed under vacuum, 0.4 g of yellow powder of RAFT agent **4** was obtained (80% yields). ^1H NMR (400 MHz, CDCl_3 , δ , ppm) 0.88 (t, 3H, CH_3), 1.25–1.69 (m, 20H,

CH_2), 1.69 (s, 6H, CH_3), 3.13 (s, 2H, CH_2), 3.28 (t, 2H, CH_2), 3.49 (s, 2H, CH_2). ^{13}C NMR (100 MHz, CDCl_3 , δ , ppm) 14.58, 23.14, 25.77, 28.08, 29.44, 29.57, 29.80, 29.92, 30.02, 30.08, 32.36, 37.74, 39.02, 40.49, 57.29, 175.75, 221.92.

Synthesis of RAFT-PZLLys-PASP

To a flame dried and argon purged schlenk tube, 0.12 g (0.23 mmol) RAFT agent **3** was added under the protection of argon, followed by the addition of 10.0 mL of DMF, and the system was

cooled down to 0 °C, and then 40 µL (0.23 mmol) DIEA was added, and the mixture was stirred for 20 min. Next, 0.68 g (2.2 mmol) ZLLys-NCA was added using its DMF solution, and the reaction was carried out for 3 days under 0 °C under mild stirring. After the NCA monomer was polymerized completed (FT-IR tracing), 0.1 g (0.46 mmol) of di-*tert*-butyl dicarbonate was added and the reaction was continually carried out overnight to protect the terminal amine group. Then, the product was added into 100 mL cool ethyl ether to get precipitate, and it was removed again in DMF for dialysis. At the end, 0.9 g product with light yellow was obtained, and the yield is 83%.

Synthesis of POGEA-PZZLys-PAsp

1.95 g OGEA (4.06 mmol) and 0.5 g (0.1 µmol) PZZLys-PAsp were dissolved into 2 mL of DMF in a Schlenk tube under stir, and 100 µmol DMF containing of 3.3 mg AIBN was added, then the mixture was subjected to three frozen–pump–thaw circles to remove any dissolved oxygen, sealed and heated to 80 °C under stirring for 12 h. After the polymerization, the solution was cooled to terminate the reaction. Purification of the sample was done by dialysis against water. 1.9 g products were obtained after removing water by freeze-drying, and the yield is 78%.

Synthesis of polymer 8

1.5 g (75.4 µmol) POGEA-PZZLys-PAsp was dissolved in 5.0 mL DMF, then 0.48 g (4.53 mmol) hydrazine dihydrochloride and 1.55 mL *N,N*-diisopropylethylamine were added sequentially, next the mixture was stirred at 45 °C for 36 h till the suspension became clear. Purification of the sample was performed by dialysis against water. 1.2 g products were obtained after removing water by freeze-drying, and the yield is 83%.

Synthesis of polymeric prodrug 9

1.0 g (5.2 µmol) of polymer 8 and 30 mg doxorubicin hydrochloride were added into a Ar gas protected dried round bottom flask (25 mL), and 5.0 mL DMF was added as solvent, and then the mixture was stirred at 45 °C for 36 h. After reaction, purification of the sample was performed by dialysis against water. 0.61 g (60% yields) product was obtained after removing water by freeze-drying, and the context of DOX in the product is 2.9% measured by means of fluorescence spectrophotometry.

Synthesis of NIR polymeric prodrug 10

2.5 mg (2.5 µmol) aminocyanine was dissolved in 1 mL DMF, a DMF solution (1 mL) containing 0.40 mg (3.0 µmol) HOSu and 0.75 mg (3.8 µmol) DCC were added. The combined solution was stirred at dark for 24 h, followed by adding into 2 mL DMF containing of 300 mg (1.5 µmol) of the as-prepared polymeric prodrug 8 under strong stir, and the mixture was mildly stirred overnight at dark. After reaction, purification of the sample was performed by dialysis against water for 48 h. 242 mg (81% yields) product was obtained after removing water by freeze-drying.

Preparation of NIR polymeric prodrug 10 micelle

The micelle was prepared by dissolving 4 mg polymer into 1 mL DMF, the obtained solution was sealed into dialysis bag and dialyzed against water to remove DMF and allow the formation of micelle.

Characterization

¹H NMR spectra were to measured on a Bruker AC 300 or 400 spectrometer as indicated. Deuterated dimethyl sulfoxide (DMSO) or deuterated chloroform containing 0.03 v/v % tetramethylsilane (TMS) was used as the solvent. FT-IR spectra were measured on a Bruker EQUINOX 55 Fourier transform infrared spectrometer using the KBr disk method. Size and size distribution of the nanogels were determined by dynamic light scattering (DLS) carried out on a Malvern Zetasizer Nano ZS90 with a He–Ne laser (633 nm) and 90° collecting optics. Measurements were performed at room temperature and the data were analyzed by Malvern Dispersion Technology Software 4.20. Fluorescence measurements were carried out on a Shimadzu RF-5301 PC Fluorescence spectrophotometer with an excitation and emission slit width of 5 and 10 nm, respectively. UV-vis spectra were obtained on a Shimadzu UV-2401PC Ultraviolet spectrophotometer. Molecular weights of the samples were determined by Gel Permeation Chromatography (GPC) equipped with two columns (one Shodex GPC KD-804 column and one guard column), a refractive index detector (RID-10A), DMF was used as the mobile phase and the measurement was performed at 30 °C at a sample concentration of 3 mg mL⁻¹. Monodispersed polystyrene standards were used for the calibration of M_n , M_w and M_w/M_n .

Molar extinction coefficient of the sample was determined by Beer's law based on three separate measurements. The relative fluorescence quantum yield was determined by using the following equation:⁴³

$$\Phi_{F(x)} = (A_s/A_x)(F_x/F_s)(n_x/n_s)^2\Phi_{F(s)}$$

where Φ , A and n refer to the quantum yield, absorption and refractive index of the solvents used. $F(x)$ stands for the area under the emission curve. Subscripts x and s represent sample and stander, respectively. Indocyanine green (ICG) was used as a reference standard with a quantum yield of 0.078 in MeOH.⁴⁴

In vitro drug release

Drug release behavior of the NIR polymeric prodrug was evaluated under both acidic and neutral condition. For the neutral condition, 400 µL NIRF prodrug solution (1 mg mL⁻¹) was sealed into a dialysis bag, which was then immersed into 50 mL 0.2 M phosphate buffered saline (PBS) solution, release experiment was conducted at 37 °C on a shaking bath. 2 mL samples were removed at predetermined time points and 2 mL fresh PBS was added at the same time. Drug released was quantified by using fluorospectrophotometer at an emission wavelength of 557 nm with an excitation wavelength of 480 nm. For the acidic condition, a similar method was employed except for 0.2 M acetate buffer was employed as the release media.

Cytotoxicity

Cytotoxicity of both the NIR polymeric prodrug was evaluated with a methyl tetrazolium (MTT) viability assay against Hela cell. Hela cells were seeded in a 96-well plate with a cell number of 5000 cells per well. A 1640 solution containing 10% fetal bovine serum (FBS) was used as the cell culture media. After incubated at 37 °C for 24 h under a 5% CO₂ atmosphere, the culture media was replaced with a series of nanogel solution (in 1640 media containing 10% FBS) ranging from 0 to 0.25 mg mL⁻¹. Then the cells were incubated at 37 °C for 2 days, and the culture media was removed and 100 μL fresh 1640 (10% FBS) was added to each well, followed by the addition of 25 μL MTT stock solution (5 mg mL⁻¹). 100 μL extraction buffer (20% SDS in 50% DMF, pH 4.7, prepared at 37 °C) was added to each well after an additional incubation of 2 h. The obtained solution were incubated overnight, the absorbance of the solution was measured at 490 nm using a Bio-Rad 680 microplate reader. The cell viability was normalized to of Hela cells cultured in complete culture medium.

Results and discussion

The combine of RAFT and ROP techniques provides many changes to design and synthesis of novel copolymers, especially multi-functional block copolymers. Here, the target copolymer was prepared as a route described in Scheme 1. RAFT agent 1 can be obtained commercially and directly used as the feed stock, and after it was activated with HOSu and DCC in CH₂Cl₂, it can reacts easily with *N*-Boc-ethylenediamine to form RAFT agent 3, after it was deprotection by trifluoroacetic acid, an amide terminal RAFT agent 4 was formed, where the amide group is the efficient initiator for ROP of NCA monomers while the tri-thioester structure used for the controlled polymerization of acrylate monomers.

Next, RAFT agent 4 was used to initiate the ROP polymerization of ZLLy-NCA at first, and then the Asp-NCA sequentially to form a diblock linear polypeptide. The choice of ZLLy-NCA and Asp-NCA mainly depends on the side chains reactive groups for the potential reaction to both NIR probe or pH-responsive linkage. Both the ROP of NCA monomers were carried out at 0 °C to avoid the active monomer mechanism (AMM) that result in the bad controlling of the polymerization.

The as-prepared diblock of polypeptide with a RAFT segment was used as the chain transfer agent for the RAFT polymerization of a macro-monomer OGEA using AIBN as initiator to induce PEG chains into the copolymer. Then, the copolymer conjugated with NIR probe (Cy 7,7) and DOX by covalent, while the linkage between DOX and copolymer is the pH-sensitive hydrazine group.

Synthesis of RAFT-PZLLys₁₀

RAFT-PZLLys was synthesized by the ring-opening polymerization of ZLLys-NCA using the RAFT agent 4 as the initiator. Fig. 1 shows the ¹H NMR spectrum of the product. Chemical shift at 7.3 ppm (C₆H₅CH₂-) and (C₆H₅CH₂-) could be attributed to the protons of the Cbz group, chemical shift at 1.5 ppm

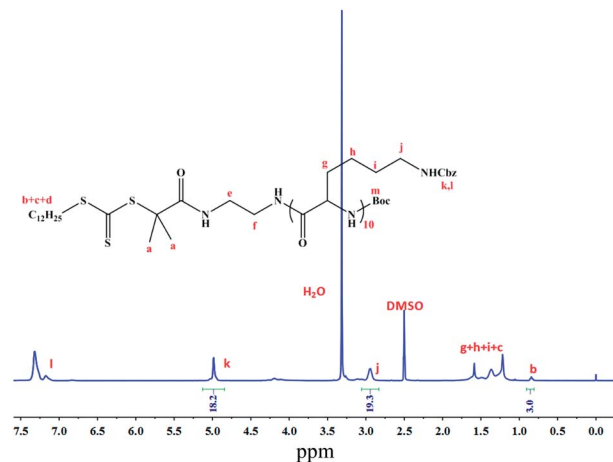


Fig. 1 ¹H NMR spectrum of RAFT-PZLLys.

(-CH₂)₃-Cbz) can be assigned to the protons of two methylene groups adjacent to the Cbz group, while chemical shifts at 2.9 ppm (-CbzNH-CH₂-) could be assigned to protons of methylene groups adjacent to amino nitrogen atom connected to Cbz group, respectively. Chemical shifts corresponding to the methyl and methylene groups of RAFT agent could be observed at 0.8 ppm (CH₃(CH₂)₁₁-) and 1.2 ppm (CH₃(CH₂)₁₁-), respectively. Molecular weight (*M_w*) of the product was determined by the integration ratio of peak b to k is 3 : 19, close to the theoretical value, indicating the polymer degree is 10.

Synthesis of RAFT-PZLLys₁₀-PAsp₁₀

Diblock copolymer RAFT-PZLLys-PAsp was synthesized by sequential ring-opening polymerization of Asp-NCA by the RAFT-PZLLys. The ¹H NMR spectrum of the diblock copolymer was shown in Fig. 2. Except for those chemical shifts corresponding to RAFT agent 4 and RAFT-PZLLys, new chemical shifts relevant to the methylene groups in the side chain of Asp (-CH₂-OBzl) could be observed at 2.8 ppm. Chemical shifts corresponding to the OBzl group could be observed at 7.3 ppm (C₆H₅CH₂-) and 5.1 ppm (C₆H₅CH₂-), and part of them overlap with the signals of Cba group. The polymeric degree of PAsp can be determined by integration ratio of relevant peaks in ¹H NMR. In Fig. 2, the integration ratio of peak j + m to k + n is 40 : 41,

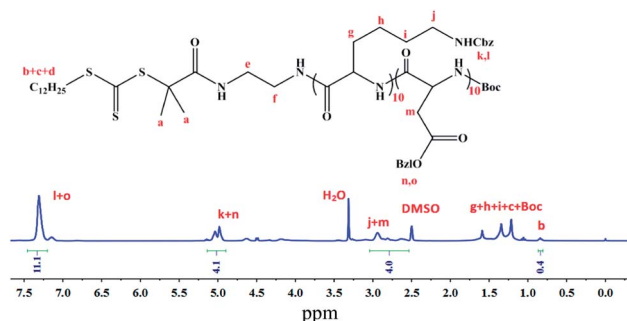


Fig. 2 ¹H NMR spectrum of RAFT-PZLLys-PAsp.

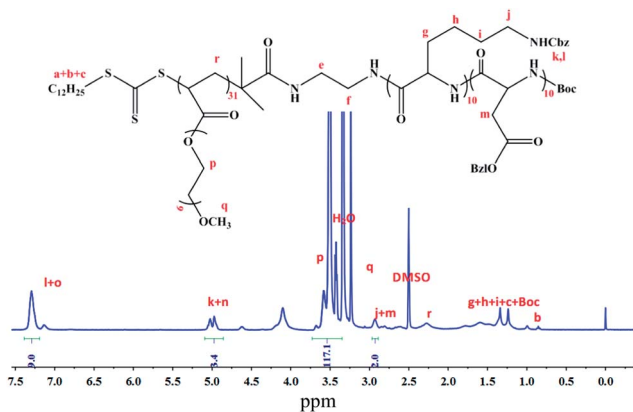


Fig. 3 ^1H NMR spectrum of RAFT-PZLLys-PAsp.

indicating that every diblock copolymer chain contains 10 Asp repeating units.

Synthesis of POGEA₃₁-PZLLys₁₀-PAsp₁₀ copolymer

Triblock copolymer POGEA₃₁-PZLLys₁₀-PAsp₁₀ was synthesized by RAFT polymerization of OGEA monomer using AIBN as initiator and RAFT-PZLLys₁₀-PAsp₁₀ copolymer as the chain transfer agent, and the polymerization was conducted for 12 h in DMF, then the unreacted monomer was removed by dialysis against water. Since the terminal amino group of RAFT-PZLLys₁₀-PAsp₁₀ may degrade the RAFT agent at 80 °C, so it was protected by the Boc group before reaction. ^1H NMR spectrum of the product was shown in Fig. 3. Characteristic chemical shifts of the POGEA block could be observed at 3.6 ppm ($-\text{CH}_2\text{CH}_2\text{O}-$) and 3.4 ppm (CH_3OCH_2-). As described above, repeating unit of the POGEA could be determined by integration ratio of the relevant peak k and p, integration ratio of the two peaks is 1 : 73, indicating the polymeric degree of OGEA is 31.

Molecular weights and weight distributions of the obtained polymers were determined by GPC, and the results were shown in Fig. 4. With each addition of the monomers, the molecular

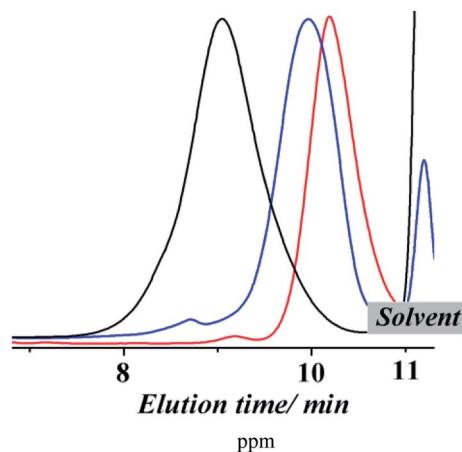


Fig. 4 GPC traces of the homopolymer, diblock copolymer and triblock copolymer in DMF.

Table 1 Molecular weights and polydispersity indexes of the obtained homopolymer, diblock and multi-block copolymer

Sample	M_w^{GPC}	M_w^{NMR}	PDI
PZLLys ₁₀	4214	3026	1.01
PZLLys ₁₀ -PAsp ₁₀	5179	4976	1.09
POGEA ₃₁ -PZLLys ₁₀ -PAsp ₁₀	25 009	19 856	1.16

weight shifts to lower elution time, indicating the propagation of the polymer chain from homogeneous polymer to multi-block copolymer. Molecular weights of the obtained samples were listed in Table 1. Polydispersity indexes of all the sample remain low (<1.2), indicating the living nature of the all polymerizations. M_w of all the samples were larger than calculated M_w from GPC, while may be due to linear polystyrenes were used for the M_w calibration.

Hydrazinolysis of the copolymer

Hydrazine dihydrochloride was used to hydrazinolysis the PAsp segment in the multi-block copolymer. ^1H NMR spectrum of the product was shown in Fig. 5. Characteristic peak of the Bzl groups locate at 7.3 ppm was decreased after deprotection, and the integration ratio of peak f to k is 1 : 1, indicating the signal at 7.3 ppm all come from the Cbz groups in PZLLys segment, and it reveals that the hydrazinolysis is complete.

Preparation of NIR probe and DOX conjugated polymer prodrug

The conjugation of DOX molecule to the copolymer was carried out in DMF by the hydrazine group, the molar ratio of DOX to the copolymer is 1 : 10 to insure the efficient reaction of DOX. The content of DOX in the copolymer can be obtained by measuring the fluorescence intensity at 557 nm ($\lambda_{\text{ex}} = 480 \text{ nm}$), and the result reveals that the context of DOX in the copolymer is 2.8 wt%.

The conjugation of NIR probe to the copolymer was also carried out by the reaction of aminocyanine-OSu with the hydrazine group. Different substitution degrees (10%, 25%, and

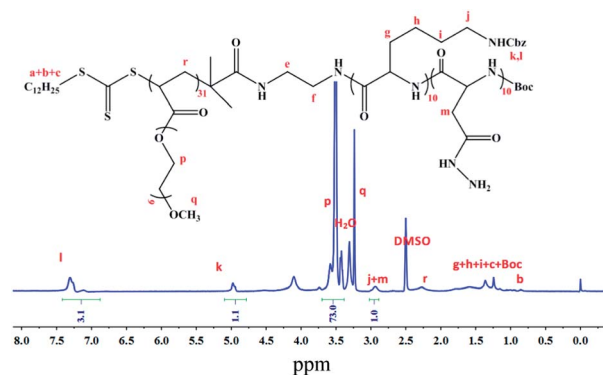


Fig. 5 ^1H NMR spectrum of hydrazine functionalized triblock copolymer in $\text{DMSO}-d_6$.

50%) of the NIR probe were synthesized, which are indicated as NIRF P1, NIRF P2 and NIRF P3, respectively.

^1H NMR spectrum of the as-prepared DOX and NIR probe conjugated copolymer is shown in Fig. 6. The signal of copolymer still preserves, while the signals for NIR probe and DOX are almost invisible, indicating the low context of them. For NIRF P1, P2 and P3, the context of NIR probe are 0.47%, 1.17% and 2.3%, respectively, which were calculated by means of fluorescence.

The as-prepared NIRF copolymers can be assembled into the micelle structure. Size and size distribution of the NIRF micelle was characterized by DLS. The results were shown in Fig. 7. The NIRF micelle has a size distribution from 60 nm to 400 nm, with an average diameter of 120 nm.

Optical property of the NIRF micelle was characterized by a the combination of UV-vis spectrophotometer and fluorescence spectrophotometer. Adsorption and emission spectra of the NIRF micelle were shown in Fig. 8. The micelle solution has two typical adsorptions at 480 nm and 675 nm, corresponding to that of DOX and NIR probe, while their emission upon

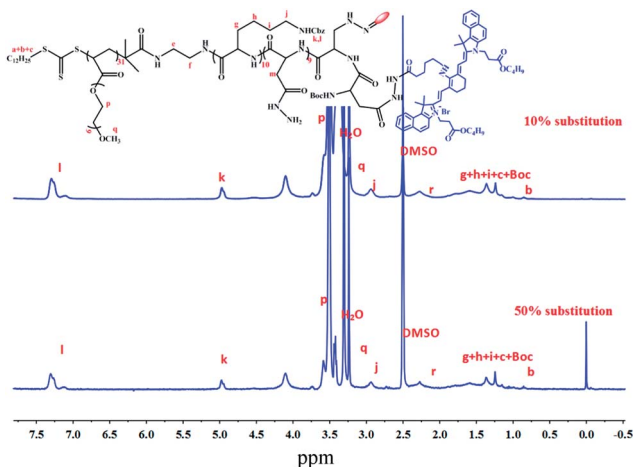


Fig. 6 ^1H NMR spectrum of NIR polymer 8 with different substitutions of NIR dye in $\text{DMSO}-d_6$.

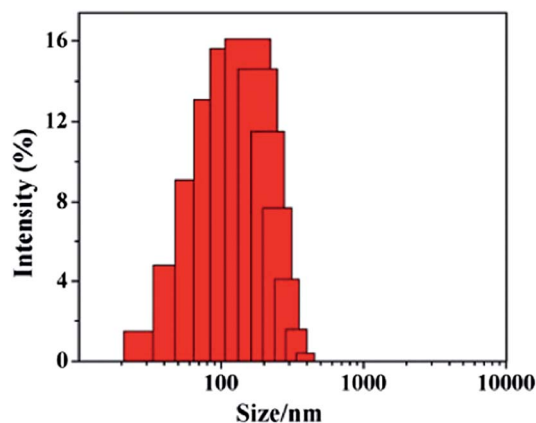


Fig. 7 Size and size distribution of NIRF polymeric prodrug 10 micelle solution (1.0 mg mL^{-1}) determined by DLS, Micelle solution was prepared by first dissolving the material and then dialysis against water.

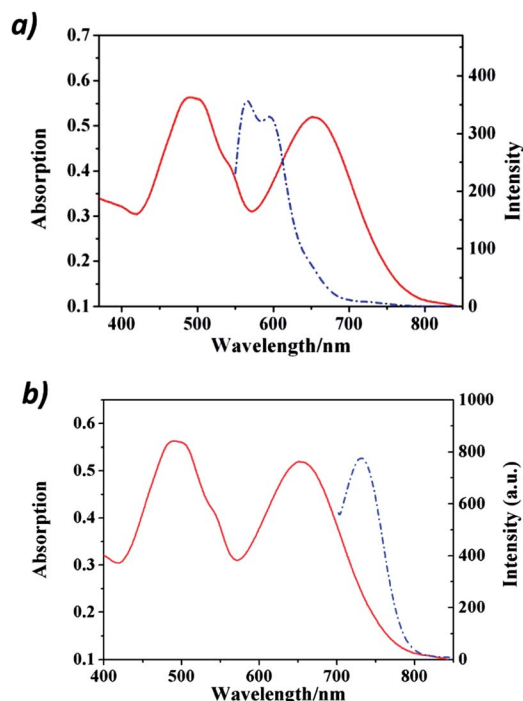


Fig. 8 Absorption (solid line) and emission (dash line) curve of NIRF P1 micelle solution (0.8 mg mL^{-1}). (a) Excited at 480 nm. (b) Excited at 650 nm, the excitation and emission slit widths were 5 and 15 nm, respectively.

excitation are 557 and 730 nm, respectively. It is worth noting that no adsorption besides 635 nm could be observed, indicating no aminocyanine aggregation took place under this condition. This may be due to the aminocyanine molecules were fixed on the polymer backbone, thus eliminated the dyes' tendency to aggregate.

Quantum yields of the NIRF micelles with different percentage of NIR dyes were determined by a standard method using ICG as reference, and the results were listed in Table 2. With increasing amount of dye molecules attached to the polymer chain, quantum yield decreases, and this could be attributed to the fluorescence resonance energy transfer (FRET) between dye molecules at higher amount of dyes.⁴⁵

In vitro drug release behavior of the NIRF prodrug was evaluated under both acidic ($\text{pH} = 5.0$) and neutral ($\text{pH} = 7.2$) condition, respectively. The results were shown in Fig. 9. Under neutral condition, a slow drug release was observed in the first 5 h, with no further release during the following 60 h, the total drug release was less than 20% in the 60 h period, while under acidic condition, an obvious acid promoted drug release behavior was observed, fast and sustained drug release could be observed during the whole time range, with near 90% drug release during the 60 h period. Accelerated drug release may be

Table 2 Quantum yields of NIRF P1, P2 and P3

Substitution	NIRF P1	NIRF P2	NIRF P3
Φ_F	0.25	0.058	0.055

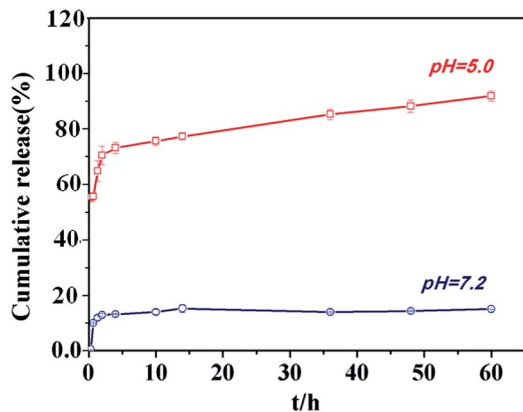


Fig. 9 Drug release behavior of the NIRF P1 at neutral (pH = 7.2) and acid (pH = 5.0) condition.

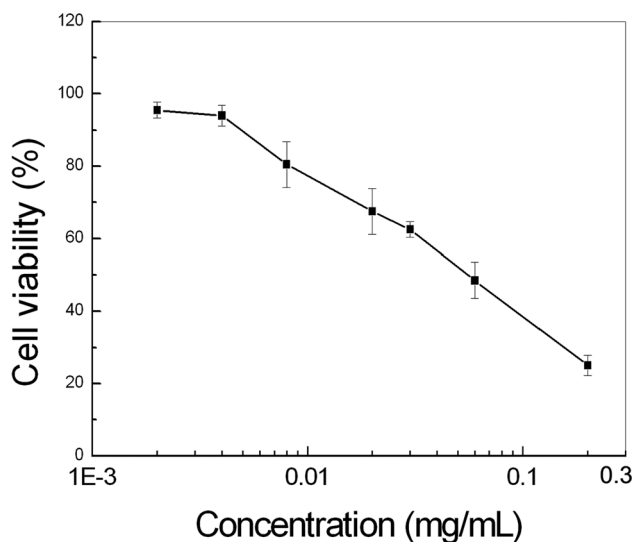


Fig. 10 Toxicity of the NIRF prodrug against Hela cell.

due to the cleavage of hydrazone bond at acidic condition, leading to the release of conjugated drug.

In vitro toxicity of the NIRF prodrug was evaluated by a MTT method. Fig. 10 shows the cell viability after incubating Hela cells with the NIRF prodrug for 72 h at various concentrations. Clearly, the toxicity of the NIRF prodrug is obvious even at low concentration (0.06 mg mL^{-1}), which could be attributed to the release of the conjugated doxorubicin in the copolymer after it was enter cell.

Conclusions

Here, both RAFT and ROP polymerization have been used to prepare a peglated multi-block copolymer of polypeptide conjugating both NIR probe and DOX molecules. The as-prepared copolymer could form micelles in size of about 120 nm, and has potential application as a NIRF polymeric prodrug for the image-guide drug delivery in cancer treatment. The obtained NIRF prodrug has strong fluorescence in the near

infrared range and could release the conjugated drug *via* pH regulation. Sustained drug cleavage from the NIRF prodrug was confirmed by *in vitro* drug release. The application of the NIRF prodrug as a theranostic agent for cell and animal experiments will be carried out in the next step.

Acknowledgements

This work is supported by the National Basic Research Program of China (no. 2011CB921403 and 2010CB923302), and the National Natural Science Foundation of China (no. 51373162). The authors would like to thank Bin Lai for his help with the MTT measurement.

Notes and references

- 1 M. E. Calderera-Moore, W. B. Liechty and N. A. Peppas, *Acc. Chem. Res.*, 2011, **44**, 1061–1070.
- 2 H. Koo, M. S. Huh, I.-C. Sun, S. H. Yuk, K. Choi, K. Kim and I. C. Kwon, *Acc. Chem. Res.*, 2011, **44**, 1018–1028.
- 3 C. Q. Ding, A. W. Zhu and Y. Tian, *Acc. Chem. Res.*, 2014, **47**, 20–30.
- 4 V. Biju, *Chem. Soc. Rev.*, 2014, **43**, 744–764.
- 5 J. J. Shi, X. Y. Yu, L. Wang, Y. Liu, J. Gao, J. Zhang, R. Ma, R. Y. Liu and Z. Z. Zhang, *Biomaterials*, 2013, **34**, 9666–9677.
- 6 S. K. Yen, D. Janczewski, J. L. Lakshmi, S. Bin Dolmanan, S. Tripathy, V. H. B. Ho, V. Vijayaragavan, A. Hariharan, P. Padmanabhan, K. K. Bhakoo, T. Sudhaharan, S. Ahmed, Y. Zhang and S. T. Selvan, *ACS Nano*, 2013, **7**, 6796–6805.
- 7 N. Erathodiyil and J. Y. Ying, *Acc. Chem. Res.*, 2011, **44**, 925–935.
- 8 C. Sun, G. Pratz, C. M. Carpenter, H. Liu, Z. Cheng, S. S. Gambhir and L. Xing, *Adv. Mater.*, 2011, **23**, H195–H199.
- 9 Z. Q. Guo, S. Park, J. Yoon and I. Shin, *Chem. Soc. Rev.*, 2014, **43**, 16–29.
- 10 L. Yuan, W. Y. Lin, K. B. Zheng and S. S. Zhu, *Acc. Chem. Res.*, 2013, **46**, 1462–1473.
- 11 H.-J. Cho, I.-S. Yoon, H. Y. Yoon, H. Koo, Y.-J. Jin, S.-H. Ko, J.-S. Shim, K. Kim, I. C. Kwon and D.-D. Kim, *Biomaterials*, 2012, **33**, 1190–1200.
- 12 R. Weissleder and V. Ntziachristos, *Nat. Med.*, 2003, **9**, 123–128.
- 13 N. Narayanan and G. Patonay, *J. Org. Chem.*, 1995, **60**, 2391–2395.
- 14 S. C. Abeylath, S. Ganta, A. K. Iyer and M. Amiji, *Acc. Chem. Res.*, 2011, **44**, 1009–1017.
- 15 J. S. Basuki, H. T. T. Duong, A. Macmillan, R. B. Erlich, L. Esser, M. C. Akerfeldt, R. M. Whan, M. Kavallaris, C. Boyer and T. P. Davis, *ACS Nano*, 2013, **7**, 10175–10189.
- 16 J. R. G. Navarro, F. Lerouge, C. Cefruga, G. Micouin, A. Favier, D. Chateau, M. T. Charreyre, P. H. Lanoe, C. Monnereau, F. Chaput, S. Marotte, Y. Leverrier, J. Marvel, K. Kamada, C. Andraud, P. L. Baldeck and S. Parola, *Biomaterials*, 2013, **34**, 8344–8351.
- 17 Y. Matsumura and H. Maeda, *Cancer Res.*, 1986, **46**, 6387–6392.

- 18 G. S. Kwon and K. Kataoka, *Adv. Drug Delivery Rev.*, 1995, **16**, 295–309.
- 19 H. Otsuka, Y. Nagasaki and K. Kataoka, *Adv. Drug Delivery Rev.*, 2003, **55**, 403–419.
- 20 T. Xing, C. Q. Mao, B. Lai and L. F. Yan, *ACS Appl. Mater. Interfaces*, 2012, **4**, 5662–5672.
- 21 X. Hu, J. Hu, J. Tian, Z. Ge, G. Zhang, K. Luo and S. Liu, *J. Am. Chem. Soc.*, 2013, **135**, 17617–17629.
- 22 H. Wang, Y. Wang, Y. Chen, Q. Jin and J. Ji, *Polym. Chem.*, 2014, **5**, 854–861.
- 23 C. D. H. Alarcon, S. Pennadam and C. Alexander, *Chem. Soc. Rev.*, 2005, **34**, 276–285.
- 24 D. Schmaljohann, *Adv. Drug Delivery Rev.*, 2006, **58**, 1655–1670.
- 25 S. Ganta, H. Devalapally, A. Shahiwala and M. Amiji, *J. Controlled Release*, 2008, **126**, 187–204.
- 26 J. Kost and R. Langer, *Adv. Drug Delivery Rev.*, 2001, **46**, 125–148.
- 27 L. Zhou, R. Cheng, H. Tao, S. Ma, W. Guo, F. Meng, H. Liu, Z. Liu and Z. Zhong, *Biomacromolecules*, 2011, **12**, 1460–1467.
- 28 Y. Bae, S. Fukushima, A. Harada and K. Kataoka, *Angew. Chem., Int. Ed.*, 2003, **42**, 4640–4643.
- 29 F. Wang, Y.-C. Wang, S. Dou, M.-H. Xiong, T.-M. Sun and J. Wang, *ACS Nano*, 2011, **5**, 3679–3692.
- 30 S. E. Paramonov, E. M. Bachelder, T. T. Beaudette, S. M. Standley, C. C. Lee, J. Dashe and J. M. J. Frechet, *Bioconjugate Chem.*, 2008, **19**, 911–919.
- 31 W. Gao, J. M. Chan and O. C. Farokhzad, *Mol. Pharm.*, 2010, **7**, 1913–1920.
- 32 K. Kataoka, T. Matsumoto, M. Yokoyama, T. Okano, Y. Sakurai, S. Fukushima, K. Okamoto and G. S. Kwon, *J. Controlled Release*, 2000, **64**, 143–153.
- 33 W. K. Moon, Y. H. Lin, T. O'Loughlin, Y. Tang, D. E. Kim, R. Weissleder and C. H. Tung, *Bioconjugate Chem.*, 2003, **14**, 539–545.
- 34 H. Lee, W. Akers, K. Bhushan, S. Bloch, G. Sudlow, R. Tang and S. Achilefu, *Bioconjugate Chem.*, 2011, **22**, 777–784.
- 35 Z. R. Zhang and S. Achilefu, *Org. Lett.*, 2004, **6**, 2067–2070.
- 36 C. Ornelas, R. Lodescar, A. Durandin, J. W. Canary, R. Pennell, L. F. Liebes and M. Weck, *Chem.–Eur. J.*, 2011, **17**, 3619–3629.
- 37 C. Ornelas, R. Pennell, L. F. Liebes and M. Weck, *Org. Lett.*, 2011, **13**, 976–979.
- 38 T. Xing, X. Z. Yang, F. Wang, B. Lai and L. F. Yan, *J. Mater. Chem.*, 2012, **22**, 22290–22300.
- 39 L. X. Liu, T. Xing, C. Q. Mao, B. Lai and L. F. Yan, *J. Macromol. Sci., Part A: Pure Appl. Chem.*, 2013, **50**, 90–98.
- 40 T. Xing, B. Lai and L. F. Yan, *Macromol. Chem. Phys.*, 2013, **214**, 578–588.
- 41 T. Xing, X. Z. Yang, L. Y. Fu and L. F. Yan, *Polym. Chem.*, 2013, **4**, 4442–4449.
- 42 W. H. Daly and D. Poche, *Tetrahedron Lett.*, 1988, **29**, 5859–5862.
- 43 J. N. Demas and G. A. Crosby, *J. Phys. Chem.*, 1971, **75**, 991–1024.
- 44 R. C. Benson and H. A. Kues, *Phys. Med. Biol.*, 1978, **23**, 159–163.
- 45 K. E. Sapsford, L. Berti and I. L. Medintz, *Angew. Chem., Int. Ed.*, 2006, **45**, 4562–4588.